2014 IEEE International Conference on Robotics & Automation (ICRA)
Hong Kong Convention and Exhibition Center
May 31 - June 7, 2014. Hong Kong, China

Experimental Evaluation of Adhesive Technologies for Robotic Grippers on Micro-Rough Surfaces

Donald Ruffatto III[1], Dzenis Beganovic[2], Aaron Parness[3], and Matthew Spenko[4]

***Abstract*— This paper presents the performance of a newly developed adhesive that combines an electrostatic adhesive with a directional dry (gecko-like) adhesive. The focus is on the adhesive's performance on micro-rough surfaces, which has a large number of applications in robotic mobility and manipulation such as climbing, perching, and grasping. Performance was characterized using shear/normal adhesion pressure limit curves and comparing the new hybrid adhesive to each individual adhesive mechanism and a control. Results show that the electrostatic directional dry adhesive generally performs better than a directional dry adhesive, but that on several surfaces, an electrostatic adhesive with no fibrillar mechanism performs the best. Additionally, the paper introduces a new mechanism that maintains an adhesive's compliance on micro-rough surfaces while transmitting shear and normal forces to a rigid structure. The mechanism is experimentally compared to a rigid backing and a gecko-like hierarchical suspension layer. Results show that the mechanism performs the best when subjected to mainly normal loads, but a hierarchical suspension handles shear loads better.**

I. Introduction and Background

Research in attachment mechanisms for robotic grippers covers a wide range of technologies. To date, most perform well only on substrates with particular material or surface properties. For many mechanisms, such as suction [1] and gecko-like fibrillar adhesives [2], [3], this equates to very smooth surfaces (e.g glass, silicon wafers). On rough surfaces, technologies such as microspines [4] perform well. Little work to date has been done on adhering to micro-rough surfaces (e.g. painted drywall, unfinished wood).

In this paper, we present the experimental results of a new adhesive designed for a wide spectrum of real-world materials with varied roughness and material composition. Specifically, we examine a newly reported hybrid electrostatic/directional-dry adhesive (EDA, [5], see Fig. 1) that can adhere to surfaces that contain bumps, crevices, and micro-scale roughness. The paper also introduces a novel interface between the adhesive and a robot that allows EDAs to withstand both shear and normal loads, whereas previously reported results on EDAs dealt with shear loads only. The paper compares the shear/normal force limit curves of EDAs coupled with the newly described mechanism with both rigid [6] and gecko-inspired hierarchical suspension systems [7].

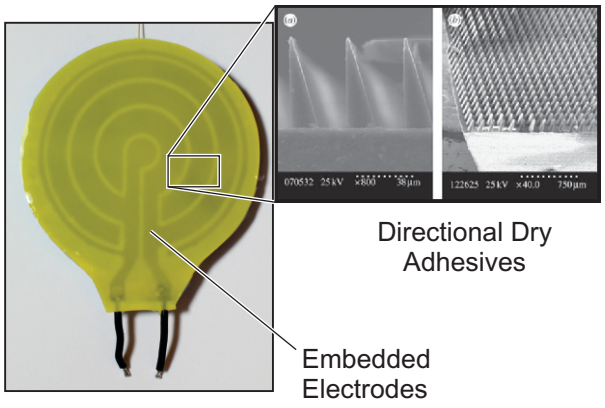

Fig. 1. The Electrostatic Directional Dry Adhesive

EDAs generate adhesion in two ways. First, they are made of a thin layer of soft, Shore 40A silicone that conforms to the substrate to create a large real area of contact with the micro-scale fibers. This helps generate large van der Waals forces. Second, the electrostatic adhesion generates a normal adhesive force [8]. Since the EDA is compliant, the normal force engages more of the EDA with the substrate, thus creating a positive feedback cycle.

On smooth surfaces, creating a large real area of contact is relatively simple. However, on rough surfaces, the adhesives need compliance. To achieve this, we previously developed a thin, highly compliant adhesive [5], [9] and demonstrated that it had comparatively high shear adhesion pressures. However, no work has been done on identifying the full shear/normal force limit curves of these adhesives. Ultimately, to effectively utilize the adhesive on a robotic platform it must have the ability to withstand normal forces. This is particularly important for applications such as robotic grappling, object manipulation, and unmanned aerial vehicle (UAV) perching. Thus, there is a disconnect between the soft, compliant structure needed to allow for a large real area of contact on a rough surface and the more rigid mounting structure needed to interface to a robot body.

One of the major issues with normal adhesion is evenly distributing the load across the entire surface. If the load is not evenly distributed, then a small area will fail and

*This work was supported by ONR grant #N00014-10-1-0769 and a NASA Office of the Chief Technologist's Space Technology Research Fellowship.

[1]Donald Ruffatto III is with the Mechanical, Materials, and Aerospace Department, Illinois Institute of Technology, Chicago, IL USA druffatto@hawk.iit.edu

[2]Dzenis Beganovic is with the Mechanical, Materials, and Aerospace Department, Illinois Institute of Technology, Chicago, IL USA dbeganov@hawk.iit.edu

[3]Aaron Parness is with the Jet Propulsion Laboratory/CalTech, Pasadena, CA USA aaron.parness@jpl.nasa.gov

[4]Matthew Spenko is with the Mechanical, Materials, and Aerospace Department, Illinois Institute of Technology, Chicago, IL USA mspenko@iit.edu

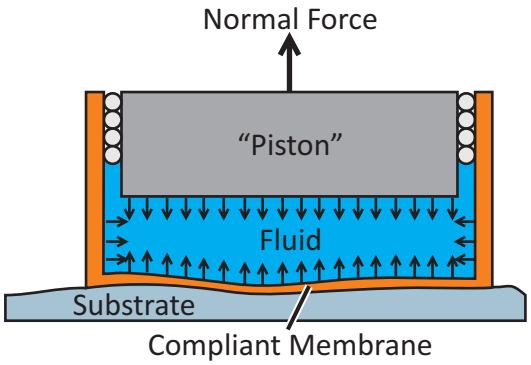

Fig. 2. Conceptual diagram of the piston mechanism used to evenly distribute normal loads to a compliant adhesive.

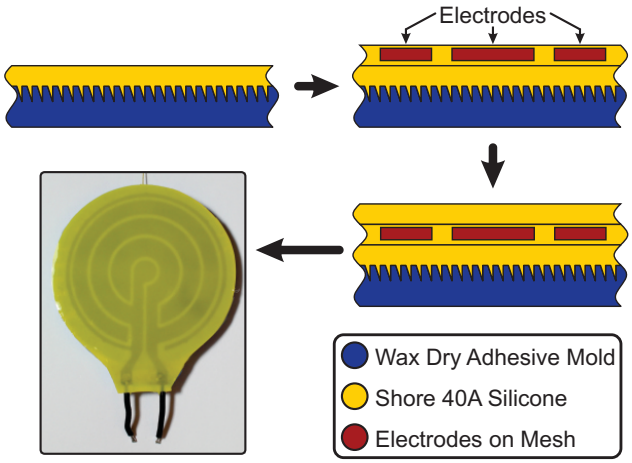

Fig. 3. Cross-sectional view of the manufacturing process for an EDA.

crack propagation will occur. Gecko-like fibrillar adhesives are designed to mitigate crack propagation [10], but so far there is a practical limit to their ability.

Evenly distributing a normal load across the adhesive when attached to non-contoured glass, or a similarly smooth surface, is relatively easy with a rigid backing [6]. However, as mentioned above, when the adhesives are used on a non-smooth surface, a rigid plate prevents the adhesive from creating a large real area of contact. To address this, previous researchers have taken inspiration from a gecko's hierarchical toe structure [11] and created a connecting layer between the adhesive and the robot that consists of directional fibrillar stalks (see Fig. 7) [7], [12]. The hierarchical structure has shown to work well when loaded in shear, but has limitations with increasing normal loads.

To address some of the issues with either the rigid or hierarchical backing layers, we developed a novel fluidized "pouch" that can both conform to a surface and evenly distribute normal loads. A cross-sectional view of the concept is shown in Fig. 2. Essentially, the system uses a piston to apply a normal load to a cavity filled with an incompressible fluid that evenly distributes the force across the adhesive. Coupled with this fluidized pouch is a mechanism, described later, that can distribute shear loads.

This paper presents experimental data comparing shear/normal force limit curves for these backing mechanisms on both smooth and micro-rough surfaces. We do this for four different types of adhesives: EDAs, electrostatic adhesives, directional dry adhesives, and reinforced silicone elastomer polydimethylsiloxane (PDMS). The paper first describes the experimental setup including fabrication methods of each backing and adhesive technology. We then present the test results along with a discussion of the results.

II. Fabrication and Experimental Setup

A. Adhesive Fabrication

The electrostatic adhesive fabrication process is described in [9]. It consists of embedding a conductive mesh, which contains an electrode pattern, into a soft silicone polymer. The mesh not only acts as the conductive electrodes for electrostatic adhesion but also serves as a reinforcement to evenly distribute shear loads across the adhesive. This electrostatic adhesive then functions similar to a reinforced PDMS [13] but with an added electrostatic adhesive element to provide a preload. Fabrication of an EDA was done using the same basic process with one important distinction: a wax mold containing the dry adhesive micro features is used to create the fibrillar structures.

Figure 3 shows the manufacturing for an EDA, which is described below:

1) A thin, approximately 125 μm, layer of silicone is spun onto a 75 mm wax directional dry adhesive mold. The silicone is allowed to partially cure.
2) A second thin layer of silicone is spun on top of the original, and the mesh is gently laid into the uncured silicone. The silicone is then again partially cured.
3) A final layer of silicone is spun on top to fully encapsulate the conductive electrodes and the silicone is allowed to fully cure.
4) The EDA is complete and removed from the wax mold.

Using this process, 52mm diameter adhesives samples were fabricated and bonded to three different backing structures, described below.

B. Fluid Pouch Backing

A fluid-filled backing mechanism that transfers normal loads to the adhesive through internal fluid pressure was coupled with a tail mechanism via a revolute joint as shown in Fig. 4. The tail mechanism transfers applied shear loads, F_x, to a Kevlar tendon that runs along the substrate material (see Fig. 5). Shear loads are transmitted from the tendon through a stress plate to the internal mesh that evenly distributes the force across the pad surface. Applied normal loads, F_z, are then transferred directly into the fluid filled backing pouch mechanism. This design conforms easily to

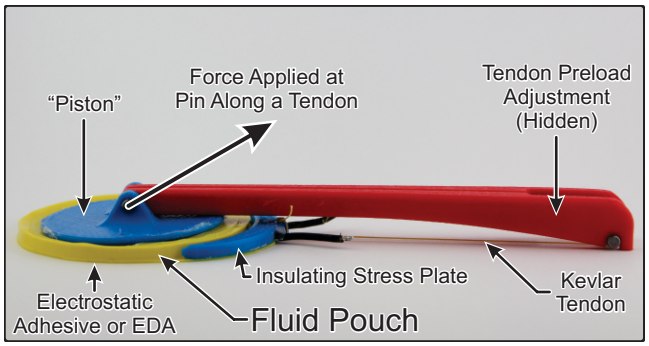

Fig. 4. Fluid-filled pouch backing with tail mechanism.

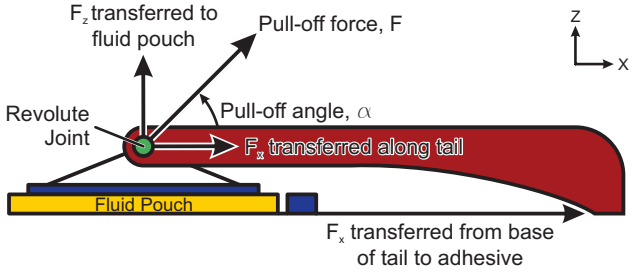

Fig. 5. Diagram showing how the applied pull-off force is transferred through the fluid pouch mechanism.

surfaces since the adhesive element is constrained only at its periphery by the silicone backing pouch and by the stiffness of the adhesive itself.

To fabricate the mechanism, a flexible cylindrical cup is cast from a Shore 40A silicone (PlatSil 73-40) using an acrylic mold. A rigid backing plate or "piston" is bonded to the silicone pouch with a silicone rubber adhesive (SilPoxy). This pouch element is then bonded directly to the back of an electrostatic adhesive or EDA. An incompressible fluid is injected into the pouch, and the pouch is vacuum degassed. For the experiments presented here, air was used due to its relative incompressibility at the tested adhesion pressures.

C. Rigid Plate Backing

The rigid plate design, shown in Fig. 6, provides direct load transfer to the adhesive and ensures that both normal

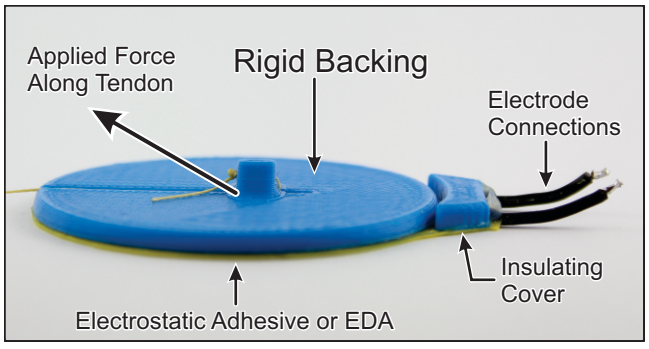

Fig. 6. Rigid plate backing.

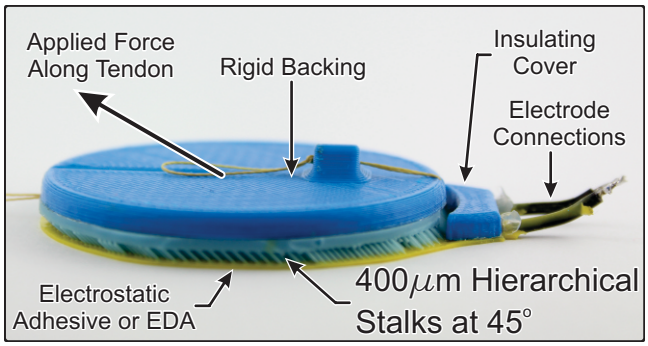

Fig. 7. Hierarchical fibrillar backing.

and shear forces are evenly distributed. However, this is at the expense of conformation at the adhesive/substrate interface level. The backing is manufactured using an FDM 3D printer and bonded with a silicone rubber adhesive (SilPoxy) to the electrostatic and EDA samples.

D. Hierarchical Fibrillar Backing

The hierarchical directional fibrillar backing is inspired by geckos and has demonstrated performance advantages on rough surfaces and when scaling adhesive patch sizes [7]. The backing layer consists of 400 μm diameter round silicone polymer stalks oriented at 45^o with respect to the adhesive (see Fig. 7). These larger stalks provide a suspension layer that allows for compliance in the normal direction while still distributing shear and normal loads.

To create the polymer stalks, a mold was fabricated by drilling 400 μm holes at 45^o through a 2.38 mm acetal sheet. This was placed into a mold cavity, filled with a shore 60A silicone (Polytek 73-60), and vacuum degassed. After the silicone was cured, the sheet of polymer stalks was removed from the mold. One side of the sheet was then bonded to a rigid backing while the stalk side was directly embedded into the back of an electrostatic adhesive or EDA. This allowed the flatness of the adhesive to be preserved.

E. Test Stage

Tests were performed on a dedicated fixture that measures both normal and shear stress generated by the adhesive (see Fig. 8). The test stage consists of a pneumatic air cylinder oriented to induce a force on the adhesives at predefined pull-off angles. For all of the performed tests a single adhesive sample was used for each adhesive/backing layer combination and no performance degradation was observed. Also, to simulate normal design operating conditions the directional dry adhesive and EDA samples were tested in their preferred direction.

The test stage is operated as follows:

1) the air slide is shifted forward and the adhesive mechanism is gently placed onto the substrate with *no preload*;
2) if required, a 5kV DC/DC converter (EMCO Q Series) activates the electrostatic element, and there is a 10 second delay;

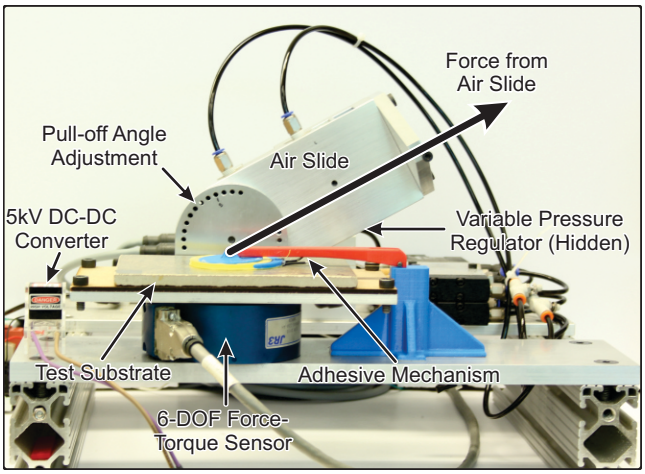

Fig. 8. Experimental test stage to evaluate shear-normal adhesion performance. The pneumatic cylinder is adjusted to apply a pull-off on the mechanism at angle ranging from 0-90^o in 5^o increments.

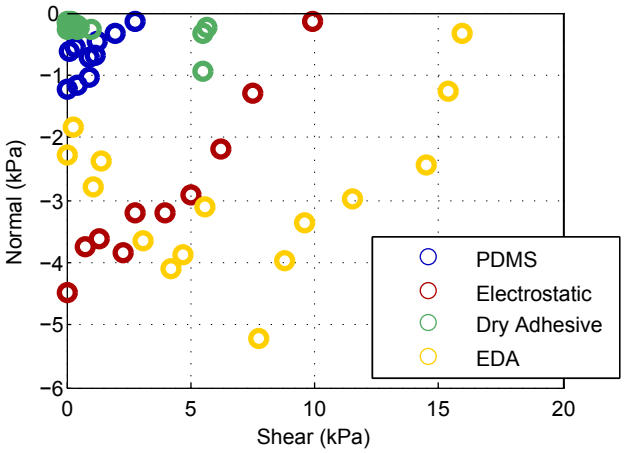

Fig. 9. Shear/normal adhesive limit curves for all four adhesive technologies: PDMS, electrostatic, directional dry, and EDA using the rigid plate backing on Tile 1, the smoothest tile. The EDA exhibits increased shear and normal adhesion compared to the other technologies.

3) the variable pressure regulator increases the force output of the air slide at a relatively slow rate of 7.8 N/s until the adhesive mechanism is detached from the substrate;
4) during the detachment phase, data from the 6-DOF force torque sensor is recorded at 2kHz using a National Instruments data acquisition board and LabVIEW;
5) after the air slide reaches the maximum set output force, 77.9 N, it is shifted back to its home position and the electrostatic element is deactivated;
6) the data is processed through a 3rd order Butterworth filter at 10Hz to remove any unrepresentative load variations due to dynamic effects; and
7) the peak normal and shear forces generated by the adhesive are extracted.

Forces are then plotted on a shear verse normal adhesion plot to give the mechanism's limit curve on that substrate. The limit curve represents the adhesive's operating range.

III. Experimental Results and Discussion

Tests were performed using the three backing mechanisms and four adhesive technologies previously described on three ceramic tiles with surface roughness from 15.7 to 28.4 μm RMS (see Table I). Roughness was measured using a profilometer along a 5 cm strip. Glass was not used due to the very high adhesion values compared to the rougher tiles and is only presented in Table I for reference. To compare the different interface mechanisms, tests are first shown for Tile 1, the smoothest. The limit curves are then shown on Tiles 2 and 3 to demonstrate the effect of surface roughness.

TABLE I
Surface Roughness of Tested Tile Substrates

Tile	Average R_a (μm)	RMS R_q (μm)	Max Profile R_t (μm)
1	12.7	15.7	81
2	18.6	23.5	121
3	23.5	28.4	136
Glass	0.16	0.19	0.83

A. Adhesive Technology

Figure 9 shows the limit curves of the four different adhesive technologies: PDMS, electrostatic, directional dry, and EDA, using a flat rigid backing on Tile 1. We chose this combination of the smoothest tile and rigid backing to isolate and highlight the differences in the adhesives.

Both the PDMS and directional dry adhesive show the lowest shear and normal adhesion, but the directional dry adhesive is notably stronger in shear. Note that these samples undergo no mechanical preload, we simply place them on the substrate. Compare those results with the electrostatic and EDA samples. The added preload generated by the electrostatic adhesive element allows for a greater portion of the PDMS and directional dry adhesive elements to contact the surface, thus creating substantially more adhesion.

The electrostatic adhesion has no directionality and the limit curve is fairly linear. On the other hand, the EDA demonstrates the typical frictional-adhesion plot [11], save one difference. At zero shear load, the EDA has some normal force. This can be eliminated if the electrostatic adhesive is turned off, thus maintaining the controllability of the adhesive. Moreover, the EDA demonstrates significantly increased adhesion compared to all other technologies.

B. Backing Mechanism

This subsection illustrates the differences in the backing mechanisms.

Figure 10 shows the limit curves for the PDMS adhesive using the three different backing mechanisms on Tile 1, the smoothest tile. Due to the lack of a preload, the rigid backing demonstrates the lowest levels of adhesion. This is because

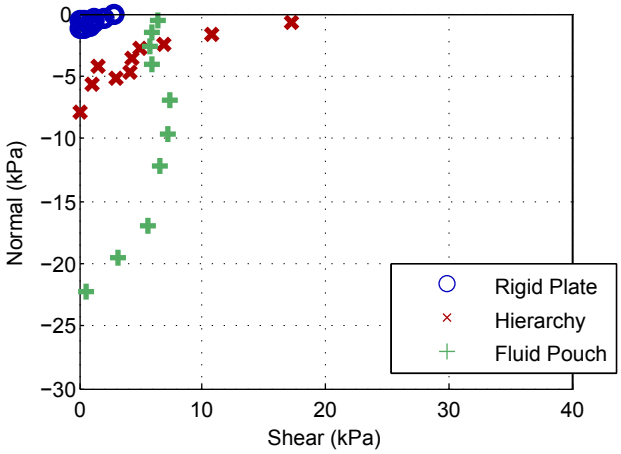

Fig. 10. Shear/normal adhesive limit curve for the three different backings using the PDMS adhesive on Tile 1, the smoothest tile. The fluid-filled pouch greatly enhances normal adhesion at the cost shear adhesion.

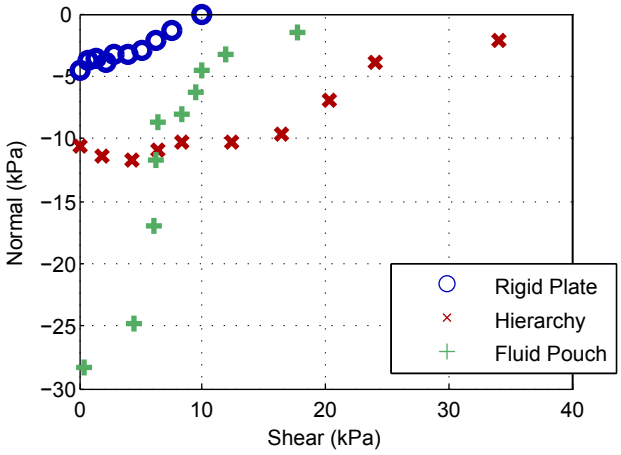

Fig. 11. Shear/normal adhesive limit curve for the three different backings on Tile 1 using an electrostatic adhesive. Compared to Fig. 10, the electrostatic adhesive increases both shear and normal adhesion.

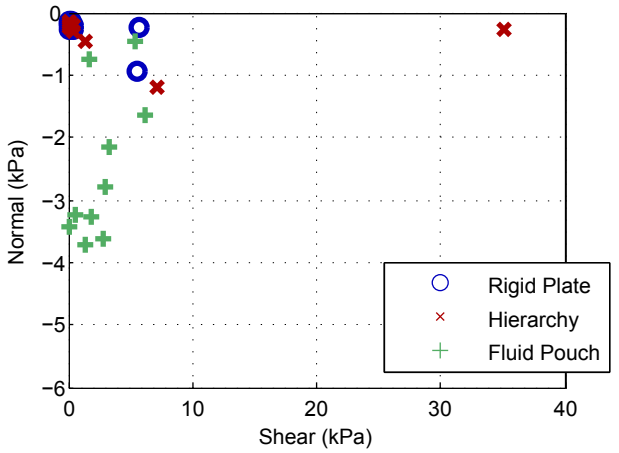

Fig. 12. Shear/normal adhesive limit curve for the three different backings on Tile 1 using a directional dry adhesive only (no electrostatic component). Without any preload, both shear and normal adhesion levels are very low.

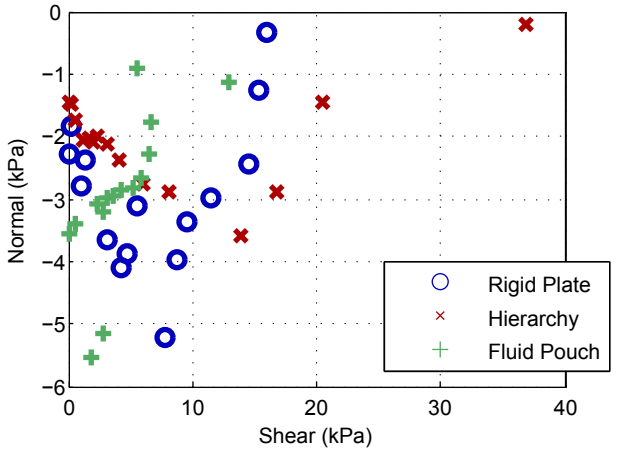

Fig. 13. Shear/normal adhesive limit curve for the three different backings on Tile 1 using an EDA. Compared to Fig. 12, there are higher levels of shear and normal adhesion. However, compared to Fig. 11, which uses electrostatic adhesion without the fibrillar stalks, there are much lower levels of adhesion.

even Tile 1 has micro-roughness that results in a low real area of contact for the rigid backing.

The hierarchical backing provides relatively high levels of shear adhesion, but low levels of normal adhesion. Conversely, the fluid pouch provides very high normal adhesion, but relatively little shear adhesion. We attribute this to inefficiencies in the tail mechanism's ability to transmit shear loads to the adhesive. Compliance in the tendon attachment points causes shear forces to inadvertently be transmitted through the pouch structure. This can cause peeling moments that may reduce overall peak adhesion.

Figure 11 is similar to Fig. 10 except for the presence of the electrostatic adhesion element. The addition of the normal preload supplied by the electrostatic adhesive element assists the PDMS in making effective surface contact. Note the greatest improvement is in the shear adhesion, which more than doubles for each type of backing mechanism.

Figure 12 shows the directional dry adhesive's performance on Tile 1 for the three different backing mechanisms. The hierarchical backing demonstrates high levels of shear adhesion, but very little normal adhesion. In this case, the normal adhesion is just slightly greater than that of the rigid plate backing. The fluid pouch again showed relatively high levels of normal adhesion with poor levels of shear adhesion.

Figure 13 is similar to Fig. 12 except that Fig. 13 uses the EDA. In this case, the EDA performs well with the rigid plate and the hierarchical suspension. However, the fluid pouch shows poor performance when used with the EDA. Again, we attribute this to the inefficient shear load transfer in the current tail mechanism design. With the EDA this is particularly important, since the EDA relies on the induced shear load to engage the directional dry adhesive stalks

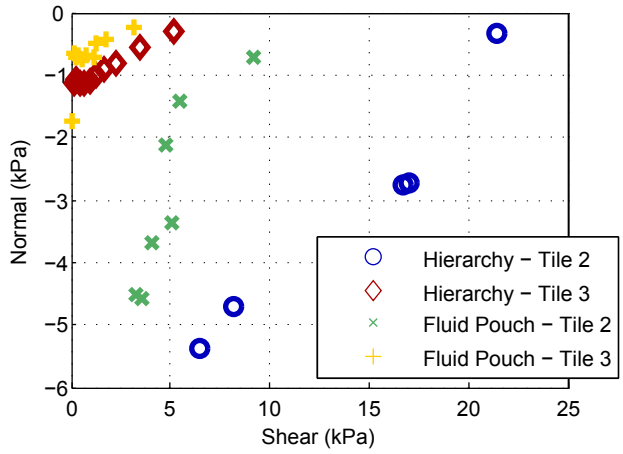

Fig. 14. Shear/normal adhesive limit curve for the electrostatic adhesive using the angled fibrillar (hierarchy) and fluid pouch backings on Tiles 2 and 3. Compared to Fig. 11, both of the technologies' performance begins to significantly decrease as the surface roughness is increased.

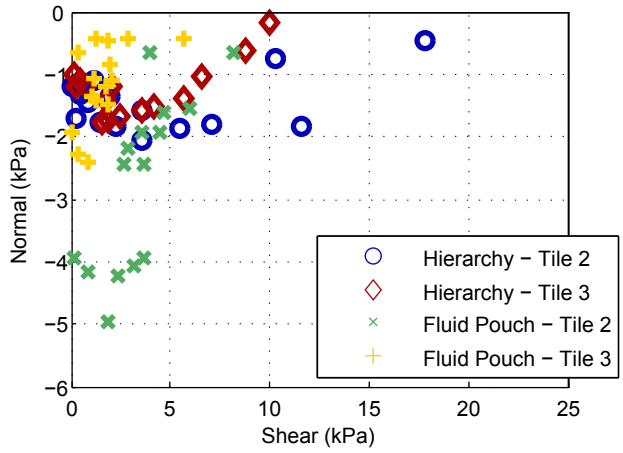

Fig. 15. Shear/normal adhesive limit curve for the EDA using the angled fibrillar (hierarchy) and fluid pouch backings on tiles 2 and 3.

with the substrate. Without proper engagement of the micro features, the performance is greatly reduced, particularly in the normal direction.

C. Surface Roughness

In this subsection, we demonstrate results on increasingly rougher surfaces. Note that we only plot the results for the hierarchical backing and fluid pouch backing since the rigid plate offers little to no adhesion on these surfaces.

Figure 14 shows the shear/normal adhesion plots for the electrostatic adhesive on Tiles 2 and 3. Although some adhesion is still present, it is significantly less than the results shown for Tile 1 in Fig. 11. Thus, while the hierarchical and fluid pouch backings do provide some levels of adhesion on rougher surfaces, there is a limit to their abilities.

Figure 15 shows the results for the EDA on Tiles 2 and 3. We originally suspected that the EDA would perform better than the electrostatic adhesive on rougher surfaces due to the fact that the stalks would be able to gain contact with the bumps and crevices in the substrate. Looking at tile 2 this is not the case; the EDA gains the frictional-adhesion profile at the expense of both shear and normal adhesion. However as the surface roughness is further increased we can see the EDA adhesive providing an advantage. On tile 3 the shear and normal performance of the EDA exceeds that of the electrostatic adhesive.

IV. Conclusion

This paper presented the shear/normal force limit curves for a newly described electrostatic directional dry adhesive on surfaces with varying degrees of roughness. The paper also introduced a new fluid-filled pouch mechanism designed to effectively transmit shear and normal loads from the EDA to a rigid structure. That mechanism was compared to two other previously reported backing designs. Results showed that the fluid-filled pouch performed better in the normal direction compared to a hierarchical suspension, but worse in shear. Future work will focus on developing a solution that provides high levels of both shear and normal adhesion as well as integrating the device into a robotic gripper for grappling and perching applications.

References

[1] S. Hirose, A. Nagakubo, and R. Toyama, "Machine that can walk and climb on floors, walls and ceilings," *5th International Conference on Advanced Robotics*, pp. 753 – 758, 1991.

[2] B. Aksak, M. P. Murphy, and M. Sitti, "Adhesion of biologically inspired vertical and angled polymer microfiber arrays," 2007.

[3] K. Daltorio, S. Gorb, A. Peressadko, A. Horchler, R. Ritzmann, and R. Quinn, "A robot that climbs walls using micro-structured polymer feet," in *Int. Conf. on Climbing and Walking Robots (CLAWAR)*, 2005.

[4] M. Spenko, G. C. Haynes, J. A. Saunders, M. Cutkosky, A. Rizzi, R. Full, and D. Koditschek, "Biologically inspired climbing with a hexapedal robot," *J of Field Robotics*, vol. 25, pp. 223–242, 2008.

[5] D. Ruffatto, A. Parness, and M. Spenko, "Improving Controllable Adhesion on Both Rough and Smooth Surfaces with a Hybrid Electrostatic/Gecko-Like Adhesive," *The Royal Society Interface*, vol. 11, 2014.

[6] E. Hawkes, E. Eason, A. Asbeck, and M. Cutkosky, "The gecko's toe: Scaling directional adhesives for climbing applications," *Mechatronics, IEEE/ASME Transactions on*, vol. 18, no. 2, pp. 518–526, 2013.

[7] A. Asbeck, S. Dastoor, A. Parness, L. Fullerton, N. Esparza, D. Soto, B. Heyneman, and M. Cutkosky, "Climbing rough vertical surfaces with hierarchical directional adhesion," in *Int. Conf. on Robotics and Automation*, may 2009, pp. 2675 –2680.

[8] G. Monkman, "Compliant robotic devices and electroadhesion," *Robotica*, vol. 10, pp. 183–185, 1992.

[9] D. Ruffatto, J. Shah, and M. Spenko, "Increasing the Adhesion Force of Electrostatic Adhesives Using Optimized Electrode Geometery and a Novel Manufacturing Process," *Journal of Electrostatics*, vol. 72, no. 2, pp. 147–155, 2014.

[10] N. Glassmaker, A. Jagota, C. Hui, W. Noderer, and M. Chaudhury, "Biologically inspired crack trapping for enhanced adhesion," *Proc. National Academy of Sciences*, vol. 104, pp. 10 786–10 791, 2007.

[11] K. Autumn, A. Dittmore, D. Santos, M. Spenko, and M. Cutkosky, "Frictional adhesion: a new angle on gecko attachment," *Journal of Experimental Biology*, vol. 206, pp. 3569–3579, 2006.

[12] H. E. Jeong, J.-K. Lee, H. N. Kim, S. H. Moon, and K. Y. Suh, "A nontransferring dry adhesive with hierarchical polymer nanohairs," *Proc Natl Acad Sci USA*, vol. 106, no. 14, pp. 5639–44, 2009.

[13] M. Bartlett, A. Croll, D. King, B. Paret, D. Irschick, and A. Crosby, "Looking beyond fibrillar features to scale gecko-like adhesion," *Adv. Mater.*, vol. 24, pp. 1078–1083, February 2012.